ORIGINAL ARTICLE

MicrobiologyOpen WILEY

Characterization and microsatellite marker development for a common bark and ambrosia beetle associate, *Geosmithia obscura*

Grace M. Pietsch[1] | Romina Gazis[2] | William E. Klingeman[1] | Matthew L. Huff[3] | Margaret E. Staton[3] | Miroslav Kolarik[4] | Denita Hadziabdic[3]

[1]Department of Plant Sciences, The University of Tennessee, Knoxville, Tennessee, USA

[2]Department of Plant Pathology, University of Florida, Homestead, Florida, USA

[3]Department of Entomology and Plant Pathology, The University of Tennessee, Knoxville, Tennessee, USA

[4]Institute of Microbiology, Czech Academy of Sciences, Prague, Czech Republic

Correspondence

Denita Hadziabdic, Department of Entomology and Plant Pathology, The University of Tennessee, Knoxville, TN, USA.
Email: dhadziab@utk.edu

Abstract

Symbioses between *Geosmithia* fungi and wood-boring and bark beetles seldom result in disease induction within the plant host. Yet, exceptions exist such as *Geosmithia morbida*, the causal agent of Thousand Cankers Disease (TCD) of walnuts and wingnuts, and *Geosmithia* sp. 41, the causal agent of Foamy Bark Canker disease of oaks. Isolates of *G. obscura* were recovered from black walnut trees in eastern Tennessee and at least one isolate induced cankers following artificial inoculation. Due to the putative pathogenicity and lack of recovery of *G. obscura* from natural lesions, a molecular diagnostic screening tool was developed using microsatellite markers mined from the *G. obscura* genome. A total of 3256 candidate microsatellite markers were identified (2236, 789, 137 di-, tri-, and tetranucleotide motifs, respectively), with 2011, 703, 101 di-, tri-, and tetranucleotide motifs, respectively, containing markers with primers. From these, 75 microsatellite markers were randomly selected, screened, and optimized, resulting in 28 polymorphic markers that yielded single, consistently recovered bands, which were used in downstream analyses. Five of these microsatellite markers were found to be specific to *G. obscura* and did not cross-amplify into other, closely related species. Although the remaining tested markers could be useful, they cross-amplified within different *Geosmithia* species, making them not reliable for *G. obscura* detection. Five novel microsatellite markers (GOBS9, GOBS10, GOBS41, GOBS43, and GOBS50) were developed based on the *G. obscura* genome. These species-specific microsatellite markers are available as a tool for use in molecular diagnostics and can assist future surveillance studies.

KEYWORDS

beetle–fungus symbiosis, Bionectriaceae, cross-amplification, detection, microsatellite markers

1 | INTRODUCTION

The genus *Geosmithia* consists of ubiquitous fungal symbionts that often are associated with wood-boring, bark, and ambrosia beetles (Huang et al., 2019; Kolarik et al., 2017). To date, almost 60 phylogenetic species have been recognized, including 21 formally described *Geosmithia* species, yet only a few of these taxa have been studied in detail (Huang et al., 2019; Kolarik et al., 2017; Strzalka et al., 2021). The distribution of *Geosmithia* species has been mapped throughout Europe (Kolařík et al., 2008; Strzalka et al., 2021) and within the Mediterranean basin (Kolařík et al., 2007). Geographic distributions are frequently supported by a close association between *Geosmithia* spp. and specific or limited diversity of ambrosia or bark beetle species (vector specificity). These relationships have provided insights into dispersal capability and the stability of the symbiotic relationship between the vector and the fungus. Although *Geosmithia* spp. can be associated with different plant hosts, Kolařík et al. (2008) suggested that host-specific communities of *Geosmithia* spp. are restricted by the range of the host plant required by the vector. Consequently, *Geosmithia* species found in one geographical area may not necessarily occur in other regions. Kolařík et al. (2007) initially identified several *Geosmithia* spp. that were only found in the Mediterranean Basin and additional *Geosmithia* spp. that were only found in Europe (Kolařík et al., 2008; Strzalka et al., 2021). This pattern of the geographic structure was carried over into studies in the western and southeastern United States in which different phylogenetic *Geosmithia* spp. were collected in each region (Huang et al., 2019; Kolarik et al., 2017). Some of the species that were originally only found in Europe have since been found in different regions of the USA (Huang et al., 2019; Kolarik et al., 2017). Looking at this comparison of the most explored regions, it is clear that some *Geosmithia* species have broad geographical distribution, whereas others so far remain limited either to regions of Europe, western United States, or Southeastern United States (Huang et al., 2019; Kolařík et al., 2008; Korlarik et al., 2017).

Many *Geosmithia* species form specialized interactions, associating only with particular ambrosia or bark beetle and their reproductive host plants. These beetle–fungus–plant host associations are consistent across North America and Eurasia (Huang et al., 2019; Kolařík et al., 2008; Korlarik et al., 2017), suggesting an ecological and evolutionary stable symbiosis. For example, *Geosmithia* sp. 26 and 27 are only found on bark beetles feeding on Pinaceae hosts, but these taxa can be found both in Europe and in the western United States (Kolarik et al., 2017); *G. ulmacea* is found only in *Ulmus* spp. (Elm) in both Europe and the western United States (Kolařík et al., 2008; Korlarik et al., 2017). In contrast, more generalized interactions occur with *Geosmithia* spp. that can survive outside bark beetle galleries and that tend to associate with many different putative arthropod vectors, such as polyphagous bostrichid beetles, which have a broader plant host spectrum than bark beetles (Kolařík et al., 2007; Kolarik et al., 2017). A number of generalist *Geosmithia* species, including *G. flava* and *G. putterilli*, are found both in Eurasia and North America. Others, however, are only found in Eurasia (i.e., *G.* sp. 1) or

North America (i.e., *G.* sp. 41) (Huang et al., 2019; Kolarik et al., 2017). *Geosmithia flava* and *G. pallida* sp. 5 can survive on both gymnosperm and angiosperm hosts (Kolarik & Jankowiak, 2013). *Geosmithia* sp. 12, which was reported initially to associate with one host plant genus (Kolařík et al., 2008), has since been isolated from a broader range of host plants than was originally recognized (Huang et al., 2017, 2019; Kolarik et al., 2017). Geographic range and beetle/host plant association concepts are subject to constant reevaluation as researchers explore more regions and identify more fungi–beetle–host interactions.

Although most *Geosmithia* species are nonpathogenic, a few are recognized as causal agents of diseases in hardwoods (Kolarik et al., 2011; Lynch et al., 2014). Tisserat et al. (2009) found an unidentified *Geosmithia* species in reproductive galleries formed by the walnut twig beetle, *Pityophthorus juglandis* (Blackman), in black walnut (*Juglans nigra* L.). The fungal species, which was later described as *Geosmithia morbida* (Kolarik et al., 2011), causes tree decline and eventual death of infected trees, a disease known as Thousand Cankers Disease (TCD) (Kolarik et al., 2011). Research to characterize *G. morbida* has identified multiple haplotypes using the internal transcribed spacer (ITS) and beta tubulin sequences (Freeland, 2012), microsatellites (Hadziabdic et al., 2014), and multilocus sequence typing with microsatellites (Zerillo et al., 2014). Freeland (2012) examined 141 *G. morbida* isolates collected in nine states and identified 12 unique haplotypes clustered in four clades. Hadziabdic et al. (2014) identified 52 haplotypes that grouped into two main genetic clusters, based on 62 isolates from four states. This sample size was expanded to 197 isolates from 12 states by Zerillo et al. (2014), who identified four main genetic clusters, which were best described using a three-region geographic model. In all cases, multiple haplotypes were often found in the same tree. Due to the importance of this fungal species as the causal agent in TCD, the *G. morbida* genome was sequenced by Schuelke et al. (2016), and simple-sequence repeat (SSR) markers were developed to characterize the populations, and easily identify and detect *G. morbida* from a diversity of substrates (Hadziabdic et al., 2011).

In 2014, the second species of *Geosmithia* was found to induce cankers in a susceptible host plant (Lynch et al., 2014). Originally identified as *G. pallida*, the recovered fungus was associated with the western oak bark beetle, *Pseudopityophthorus pubipennis* Swaine, infesting coastal live oak, *Quercus agrifolia* Née trees in California. The disease caused by this fungus was named Foamy Bark Canker disease (Lynch et al., 2014). Subsequent genetic examination of the fungus resulted in a reclassification of the causal fungal agent as belonging to the unnamed lineage *G.* sp. 41 (Kolarik et al., 2017). *Geosmithia* sp. 41 has been isolated from beetle galleries in a wide range of host plants in the western United States (Kolarik et al., 2017), and beetles extracted from two additional host plants in the southeastern United States (Huang et al., 2019). To date, this fungal species has only been reported to induce disease symptoms in *Q. agrifolia* (Lynch et al., 2014).

Geosmithia obscura (Kolarik et al., 2005) was first isolated and characterized from *Scolytus* spp. beetles in Europe. Since then, this

fungal species has been found infrequently, in both the USA and Europe, occurring in association with various bark beetles (Huang et al., 2019; Kolařík et al., 2008; Kolarik et al., 2017; Six et al., 2009). During an insect screening survey for _G. morbida_ within TCD-compromised habitats in Knox and Blount Counties, Tennessee, several additional _Geosmithia_ species, including _G. obscura_, were isolated from bark and ambrosia beetles, including _Cnestus mutilatus_ (Blandford) and _Xylosandrus crassiusculus_ (Motschulsky) and the bostrichid beetle _Xylobiops basilaris_ (Say), which were collected adjacent to walnut tree canopies (Chahal et al., 2017; Six et al., 2009). Greenhouse assays were performed to determine the pathogenicity of the above-collected isolates to black walnut (_Juglans nigra_ L.). Of these, an isolate of _G. obscura_ recovered from a specimen of _X. crassiusculus_ was able to induce cankers. Even though only inoculated branches showed canker symptoms, Koch's postulates were not fulfilled, as we were unable to recover the isolate from sapwood tissue surrounding the lesions through culture-based techniques. Although _G. obscura_ associations with bark and ambrosia beetles have been documented in other locations (Huang et al., 2019; Kolarik et al., 2005; Kolařík et al., 2008), host plant associations and consequences of the interaction remain largely undescribed.

To address this knowledge gap and to provide a methodology by which _G. obscura_ DNA can be detected from potential vector insects or within host plant tissues, the objectives of this study were (1) to identify, develop, and characterize _G. obscura_ microsatellite markers using genomic data and (2) to determine the specificity of the newly developed markers for their use as a diagnostic tool.

2 | MATERIALS AND METHODS

2.1 | Genome sequencing, assembly, and microsatellite development

For whole-genome sequencing, DNA from _G. obscura_ isolate 6BE2, which originally was cultured from body wash samples from an _X. crassiusculus_ beetle live-trapped in eastern Tennessee (Chahal et al., 2019), was extracted using Qiagen Blood and Cell Culture DNA Kit Maxi (Qiagen), according to the protocol (Gazis et al., 2016). Libraries were prepared at the Michigan State University Genomics Core lab (https://rtsf.natsci.msu.edu/genomics/) using the Illumina TruSeq Nano DNA Library Preparation Kit on a PerkinElmer Sciclone G3 robot following the manufacturer's recommendation. Completed libraries were checked for quality (QC) and quantified using a combination of Qubit dsDNA HS and Caliper LabChipGX HS DNA assays. All libraries were pooled in equimolar amounts based on QC and quantified using the Kapa Biosystems Illumina Library Quantification qPCR Kit. Library sequencing was performed with Illumina HiSeq 4000 flow cell using a 2×150 bp paired-end format and a HiSeq 4000 SBS Reagent Kit. Base calling was completed using Illumina Real-Time Analysis (RTA) v2.7.6 and the output of RTA was demultiplexed and converted to FastQ format with Illumina Bcl2fastq v2.19.0.

TABLE 1 Summary of microsatellite markers used for identification and cross-amplification of _Geosmithia obscura_ and _Geosmithia_ spp. isolates.

Total number of sequences	5752
Number of sequences with at least one microsatellite locus	1653
Total number of microsatellite loci identified	3256
Number of compound microsatellite loci[a]	94
Number of microsatellite loci with primers[b]	2815
Dinucleotide (min. 8 repeats) with primers	2011
Trinucleotide (min. 7 repeats) with primers	703
Tetranucleotide (min. 6 repeats) with primers	101

[a]Compound microsatellite loci are defined as any microsatellite loci next to each or separated by less than 15 bases.
[b]No primers are designed for compound microsatellites.

The transcript quality of these reads was assessed using FastQC (Andrews, 2010) and error correction was performed using default values with Bloom Filter Correction (Li, 2015). Using the trimming program, Skewer (Jiang et al., 2014) adapter sequences were removed and reads were filtered by requiring a minimum quality score of 20 in at least 70% of the bases. Except for minimal read length after trimming set to 30, all default parameters were used. Next, the transcripts were assembled using Assembly By Short Sequences (ABySS), specifically its paired-end option, abyss-pe, using a _k_-mer size of 81 and default settings for all other options (Simpson et al., 2009). Finally, sequences were masked for low complexity regions with Dustmasker (level of 1) (Morgulis et al., 2006).

Microsatellite markers were identified with a custom Perl script (Staton & Ficklin, 2018) (Table 1). This script utilizes Primer3 (Rozen & Skaletsky, 2000) to search for di-, tri-, and tetra-repeating motifs, with primer product sizes ranging between 100 and 250 base pairs (bp) long (Untergasser et al., 2012). This script also produced text files containing the IDs and forward and reverse primers for the identified markers; these would be used to identify common regions between the different species' genome scaffolds.

2.2 | Fungal strain selection, DNA extraction, amplification, and molecular confirmation

Following Gazis et al. (2018) protocol, axenic cultures from seven _G. obscura_ isolates and 18 additional isolates of _Geosmithia_ species (Table 2) were placed onto Difco™ Potato Dextrose Broth (Becton, Dickinson and Company) at 22°C for up to 2 weeks, after which mycelium was harvested for DNA extraction. For species confirmation, GeneJet Genomic DNA Purification Kit (Thermo Fisher Scientific) was used, following the manufacturer's protocols with slight modifications. These modifications included increased proteinase K to 40 µl/sample and an extended overnight incubation period at 56°C. Samples were quantified using a NanoDrop 1000

TABLE 2 Geosmithia species used to assay cross-amplification of Geosmithia obscura microsatellite markers.

Species and isolate code	Collector/collection	Blast ID	Coverage	Similarity	GenBank accession no.
Geosmithia lavendula CBS344.49	Centraalbureau voor Schimmelcultures (CBS)	N/A[a]	N/A	N/A	N/A
G. lavendula	Fungal culture collection	*Geosmithia lavendula* strain CCF4336	100%	100%	MG733658.1
Geosmithia morbida GM10	Vito/Windham	*Geosmithia morbida* isolate GM-TN-SP2	100%	99%	MG008848.1
G. morbida GM17	Vito/Windham	*Geosmithia morbida* isolate GM-TN-SP1	100%	100%	MG008847.1
G. morbida GM182	Hadziabdic Lab	N/A	N/A	N/A	N/A
G. morbida GM246	Hadziabdic/Nix	*Geosmithia morbida* isolate GM236	100%	100%	MG008837.1
G. morbida GM249	Hadziabdic Lab	N/A	N/A	N/A	N/A
G. morbida GM250	Hadziabdic Lab	N/A	N/A	N/A	N/A
Geosmithia obscura 6BE2	Chahal	*Geosmithia obscura* isolate Hulcr 18146	100%	100%	MH426774.1
G. obscura 14MCE1	Hadziabdic Lab	N/A	N/A	N/A	N/A
G. obscura 18BS1	Chahal	*Geosmithia obscura* isolate Hulcr 18146	100%	100%	MH426774.1
G. obscura 18ME3	Chahal	*Geosmithia obscura* isolate Hulcr 18146	100%	100%	MH426774.1
G. obscura CBS121749	Centraalbureau voor Schimmelcultures (CBS)	N/A	N/A	N/A	N/A
G. obscura CCF3422.1	Kolarik	*Geosmithia obscura* isolate Hulcr 18146	100%	100%	MH426774.1
G. obscura CCF3423.1	Kolarik	*Geosmithia obscura* isolate Hulcr 18146	100%	100%	MH426774.1
G. obscura CCF3424.1	Kolarik	*Geosmithia obscura* isolate Hulcr 18146	100%	100%	MH426774.1
G. obscura CCF3425.1	Kolarik	*Geosmithia obscura* isolate Hulcr 18146	100%	100%	MH426774.1
Geosmithia pallida 6LN5	Chahal	*Geosmithia pallida* genomic DNA, strain U112	100%	100%	HF546259.1
G. pallida 9730	Hulcr	*Geosmithia* cf. *pallida* sp. 2 YTH-2018 isolate Hulcr 17357	100%	99%	MH426761.1
G. pallida 9737	Hulcr	*Geosmithia* cf. *pallida* sp. 2 YTH-2018 isolate Hulcr 17357	100%	99%	MH426761.1
G. pallida CBS260.33	Centraalbureau voor Schimmelcultures (CBS)	N/A	N/A	N/A	N/A
Geosmithia putterilli NRRL 2024	Hulcr	*Geosmithia putterilli* genomic DNA, strain U83	100%	100%	HF546348.2
Geosmithia sp. 2 LS1XB	Chahal	*Geosmithia pallida* genomic DNA, strain U112	100%	100%	HF546259.1
G. sp. 2 K1W1	Chahal	*Geosmithia pallida* genomic DNA, strain U112	100%	100%	HF546259.1
G. sp. 2 3BHS13	Chahal	*Geosmithia pallida* genomic DNA, strain U112	100%	100%	HF546259.1
G. sp. 10 11LE1	Chahal	*Geosmithia omnicola* isolate Hulcr 17349	100%	99%	MH426757.1
G. sp. 21 LS5XB	Chahal	*Geosmithia* sp. 21 NL-2014 strain MK1665	100%	100%	KF808310.1
G. sp. 23 4LW11	Chahal	*Geosmithia* cf. *pallida* sp. 23 YTH-2018 isolate Hulcr 17359	99%	100%	MH426765.1

TABLE 2 (Continued)

Species and isolate code	Collector/collection	Blast ID	Coverage	Similarity	GenBank accession no.
G. sp. 23 4MN3	Hadziabdic Lab	N/A	N/A	N/A	N/A
G. sp. 41 6ME1	Chahal	Geosmithia cf. pallida sp. 41 YTH-2018 isolate Hulcr 19078	99%	100%	MH426786.1
G. sp. 41 8BN26	Chahal	Geosmithia cf. pallida sp. 41 YTH-2018 isolate Hulcr 19078	99%	100%	MH426786.1
G. sp. 41 4BE20	Chahal	Geosmithia cf. pallida sp. 41 YTH-2018 isolate Hulcr 19078	99%	100%	MH426786.1
G. sp. 41 18MN2	Chahal	Geosmithia cf. pallida sp. 41 YTH-2018 isolate Hulcr 18144	100%	100%	MH426772.1
Penicillium namyslowskii CBS686.85	Centraalbureau voor Schimmelcultures (CBS)	N/A	N/A	N/A	N/A
Rasamsonia argillacea	Hadziabdic Lab	N/A	N/A	N/A	N/A
Talaromyces viridulus CBS252.87	Centraalbureau voor Schimmelcultures (CBS)	N/A	N/A	N/A	N/A

Note: Species identification was confirmed using the RNA operon with the ITS primers ITS1F and ITS4R.

[a]N/A designates an isolate for which no live culture was available. Cross-amplification was performed on a DNA sample only; no coverage, similarity, or GenBank accession data can be provided.

Spectrophotometer (Thermo Fisher Scientific) and stored at −20°C until used. To confirm the identity of the *Geosmithia* isolates, the RNA operon was amplified and sequenced using the ITS primers ITS1F (Gardes & Bruns, 1993) and ITS4R (White et al., 1990), following Gazis et al. (2018) protocol. The polymerase chain reaction (PCR) product was visualized on a 2% agarose gel and sent to MCLAB (www.mclab.com) for cleaning and sequencing. Sequenced strands were assembled into contigs using Sequencher 5.0 (Gene Codes Corporation). Sequences were compared to the NCBI nucleotide database using BLAST search optimized to exclude uncultured/environmental sample sequences and to search sequences from type material. If species identity of 99%–100% was not obtained, an unrestricted BLAST search was performed (Table 2). Additional *Geosmithia* spp. (*G. obscura* CBS121749, *G. lavendula* CBS344.49, *G. pallida* CBS260.33) and other species (*Penicillium* [formerly *Geosmithia*] *namyslowskii* CBS686.85 and *Talaromyces* [formerly *Geosmithia*] *viridulus* CBS252.07) were acquired as DNA samples from The Dutch Centraalbureau voor Schimmelcultures (CBS) Fungal Biodiversity Centre collection or from previously verified DNA samples from our collection [*G. obscura* 14MCE1, *G.* sp. 23 4MN3, *G. morbida* GM182, *G. morbida* GM249, *G. morbida* GM250, and *Rasamsonia argillacea* (Stolk, H.C. Evans & T. Nilsson) Houbraken & Frisvad (formerly *G. argillacea*)].

2.3 | Microsatellite characterization and cross-amplification

A total of 2815 microsatellite markers were identified with flanking primer sequences. Of those, 75 microsatellite markers (consisting of 25 di-, 25 tri-, and 25 tetranucleotide sequences) were randomly selected and screened to identify polymorphic markers. For the initial characterization, all primer pairs were tested using three *G. obscura* and one *G. morbida* isolates. PCR reactions were conducted using 4 µl GoTaq G2 Hot Start Colorless Master Mix (Promega Corporation), 1 µl each forward and reverse primers, 0.5 µl dimethyl sulfoxide, 5 µl sterile water, and 1 µl genomic DNA providing a 12.5 µl sample volume. Samples were placed in a SimpliAmp ThermalCycler (Thermo Fisher Scientific) with the following protocol: 94°C for 3 min, followed by 35 cycles of denaturation at 94°C for 40 s, annealing at 55°C for 40 s, and primer extension at 72°C for 30 s, followed by 72°C for 4 min. PCR products were separated using a QIAxcel Capillary Electrophoresis System (Qiagen) with a 25–500 bp size standard. Products with a relative fluorescence unit (RFU) of 100 or greater were scored as positive amplification. Only a subset of microsatellite markers (*n* = 28) that were identified as polymorphic was further screened in the cross-amplification study. To accomplish this step, six *G. obscura* isolates along with 24 isolates from nine different *Geosmithia* species and three additional isolates outside *Geosmithia* were screened. Isolates were amplified using the PCR protocol described above and separated using the QIAxcel Capillary Electrophoresis System with an RFU value of 100 or greater

scored as positive. The number of alleles and haploid genetic diversity was obtained using the program GenAlEx 6.5 (Peakall & Smouse, 2012).

3 | RESULTS

3.1 | Microsatellite characterization and cross-amplification

ABySS assembly of 9.1 million paired sequencing reads from DNA of *G. obscura* resulted in 5752 unitigs spanning 28.9 Mb with an N50 of 24,134 and 47.4× coverage. The assembled sequences were screened for microsatellite development, from which 1653 unitigs yielded at least one microsatellite marker, resulting in 3256 candidate microsatellite markers (Table 1). From this group, we identified 94 compound microsatellites, which were either located next to each other or separated by less than 15 bp, and 2815 microsatellite markers with flanking primer sequences. Parameters for a minimum number of replicates for each motif were established at 8 for dinucleotides, 7 for trinucleotides, and 6 for tetranucleotides. Using these baseline parameters, a total of 2236, 789, 137 di-, tri-, and tetranucleotide motifs were identified, respectively, with 2011, 703, 101 di-, tri-, and tetranucleotide motifs, respectively, containing markers with primers (Table 1). We tested 75 markers for amplification and the presence of polymorphic bands. All tested markers resulted in amplification, and a total of 36 markers were polymorphic (11 di-, 13 tri-, and 12 tetranucleotides). Further optimization of the microsatellite markers yielded 28 markers with single, consistently recovered bands (Table 3), which were used to test cross-amplification of *G. obscura* markers into other *Geosmithia* species.

3.2 | Fungal strain selection, DNA extraction, amplification, and molecular confirmation

Blast results confirmed identities for the isolates of *G. obscura*, *G. morbida*, *G. lavendula*, *G. putterilli*, and *G. omnicola* (Table 2). Two species in the *G. pallida* complex were identified correctly when a general BLAST search rather than type material option was selected. With the type material search option, *G. pallida* isolates (*G. pallida* 9730 and *G. pallida* 9737) were identified as *G. brunnea* isolate CBS142633 (Table 2).

3.3 | Cross-amplification of *G. obscura* microsatellites

Microsatellite markers amplified products with a range of 4–28 bp difference in allelic class size. The smallest range was in GOBS21 with a 4 bp difference in identified alleles, while GOBS43 had the largest range in size (Table 3). Microsatellite markers were designed to

amplify *G. obscura* DNA; however, *G. argillacea* [current name *Rasamsonia argillacea* (Houbraken et al., 2012)] amplified a band of the expected fragment length with 21 of the 28 loci (Table 4). Most of the amplified fragments had an RFU value less than 500, although the fragment amplified by GOBS4 was greater than 1000 and the fragment amplified by GOBS73 was greater than 500. Initial screening amplified products of the expected size in the *G. morbida* isolate tested when using two of the 75 microsatellite markers. These two microsatellite markers were excluded from the cross-amplification screening. However, additional *G. morbida* isolates did amplify fragments in 9 of the 28 microsatellite markers (Table 4). All of these fragments had an RFU value of less than 1000. GOBS74 generated an amplicon in most of the species in the *G. pallida* complex tested (*G. pallida*, *Geosmithia* sp. 2, *Geosmithia* sp. 23, and *Geosmithia* sp. 41), with products having an RFU value greater than 2000–3000 in some cases. A total of five microsatellite markers (2 di and 3 tri) only generated amplicons in *G. obscura*. These were GOBS9, GOBS10, GOBS41, GOBS43, and GOBS50 (Tables 3 and 4).

4 | DISCUSSION

The economic and ecological damage/impact of *G. morbida* to commercial and natural populations of walnut trees and the potential damage/impact that *G.* sp. 41 can cause on oak populations, has prompted the screening of other *Geosmithia* species for pathogenic traits. Preliminary research showed canker formation in walnut trees artificially inoculated with *G. obscura*, suggesting that this species may be pathogenic. To uncover the natural distribution and host/vector association range of this species, we need to easily identify isolates that may be present on beetle vectors and in galleries using heterogeneous, environmental samples. Previous work in our lab identified SSR markers specific to *G. morbida* (Hadziabdic et al., 2011), which led to rapid and early diagnostic tools that can detect this pathogen directly from infected sapwood tissue, avoiding the need for time-consuming culture protocols (Chahal et al., 2019; Gazis et al., 2018; Oren et al., 2018; Stackhouse et al., 2021). In Gazis et al. (2018) alternative uses of microsatellites are presented that expand upon their use in traditional population genetics applications. Estimated costs associated with the processing of samples to conduct assays like the approach presented here are included within Supplemental Material reported in Stackhouse et al. (2021).

With the advent of next-generation sequencing technologies, the number of microsatellites identified in fungi has increased dramatically due to the ability to produce longer reads of DNA at a time (Cai et al., 2013; Dutech et al., 2007; Schoebel et al., 2013). At the same time, new and improved algorithms and computational capabilities for finding microsatellite regions and generating primers have become available (Cai et al., 2013; Mercière et al., 2015). Longer repeats are more likely to mutate across time, creating variation in repeat lengths, which accounts for polymorphic alleles (Dutech et al., 2007). However, even with longer reads by using 454 pyrosequencing, Schoebel, Brodbeck, et al. (2013) found few microsatellites in fungi

TABLE 3 Twenty-eight microsatellite markers were used to assay cross-amplification of *Geosmithia obscura*, a common bark and ambrosia beetle associate, to other *Geosmithia* spp.

Locus[a]	Primer sequence (5′–3′)	Repeat motif	Allelic class size range (bp)	Na[b]	h[c]
GOBS4	F: ATGCAAGTCTCCATCGGTCC	$(GA)_9$	115–122	5	0.72
	R: ATTGTCATGCGCGTGTGTGG				
GOBS9	F: TTTGTGCCTCTCTACGGTCC	$(AT)_{10}$	138–148	6	0.78
	R: TCATACCTCACACACACTCCG				
GOBS10	F: CATGCCGTTGCTATTGTCGG	$(GT)_{12}$	142–149	4	0.69
	R: TGAAGTTGGTCGGTGGATCG				
GOBS11	F: CGAGACTTTATGAGTGATTGCAGC	$(TA)_{12}$	139–144	4	0.66
	R: CTGCAGTGCCAATGGAAGC				
GOBS12	F: TGTCTCCTCACGAATGAAGGC	$(GA)_{11}$	146–157	6	0.81
	R: AGCAGCAATAGTGGCTACCC				
GOBS13	F: TTCCCACCTTGGCTCTTTCC	$(TG)_8$	156–160	5	0.72
	R: ACAGAGCAATAGATACAGAGTGC				
GOBS16	F: CTTTCGACGACTGCATTCCC	$(AT)_8$	176–181	5	0.74
	R: AGAGAACAGAAAGGTGGCCG				
GOBS18	F: GTACGAGACAAAGCGATGCG	$(CA)_{10}$	194–198	4	0.62
	R: CAGTTCGACTTCTGGGACCC				
GOBS20	F: TTTCTTGGTCGTTCCTTCCC	$(TC)_{10}$	221–226	5	0.64
	R: TTCGGTTTGTTGGTGTGTGC				
GOBS21	F: ACCATGTCTGCAGCAAGTGG	$(CT)_8$	232–235	3	0.63
	R: TGGGCAGGAGTAAAGTACGG				
GOBS26	F: TAGGGCACGGAACATGATGG	$(AAC)_8$	94–101	6	0.82
	R: GGTGAATTGGAAGGACACGC				
GOBS31	F: AACATGCTGGGCAATTGAGC	$(GGT)_{10}$	101–123	7	0.84
	R: AGTTCCGTAGCTTGTAGCCG				
GOBS38	F: GATGGTCGTAGATCCGTTCCC	$(GGT)_{10}$	159–166	6	0.81
	R: CTCTCTGTGTGTGTCGAGGG				
GOBS41	F: GCAGAGGGAGAGTATTCCGC	$(ACT)_{13}$	176–202	7	0.84
	R: TCTCAGGTTCCCAGGATCCC				
GOBS43	F: ACACTTGATTCTCCTGGCGC	$(CGG)_{10}$	190–217	6	0.82
	R: CCATGTTTCCCACATTCGCG				
GOBS44	F: CGCCTTGTGTTACAGGATCG	$(TAA)_8$	188–211	6	0.79
	R: CCAGACTCTCCAGCTTTGTGG				
GOBS45	F: TCAGCAGTAAATGGCAAATAGC	$(CAA)_{10}$	193–200	4	0.62
	R: GAATTTGATGCCCAGACCGC				
GOBS46	F: CTGAACCGAGTAATCCCGCC	$(TCC)_7$	200–220	7	0.84
	R: GCAGAAACTGGGTTATGCGG				
GOBS47	F: AGTGAGAGAGGACTGTAGGG	$(TAG)_7$	186–201	4	0.52
	R: TGTGGGCGACATATTAGGGC				
GOBS50	F: TCTTGACAGTTCGCCTCACG	$(TTC)_8$	229–235	5	0.77
	R: TGTTCCCTTGACGTTCACGG				

TABLE 3 (Continued)

Locus[a]	Primer sequence (5′–3′)	Repeat motif	Allelic class size range (bp)	Na[b]	h[c]
GOBS51	F: CAGGATGGAGCTTGGGAAGG	$(AAGA)_7$	99–111	5	0.72
	R: GGAACAGGCAAGAGCAAGGG				
GOBS53	F: CGTTGCGACATATGGTGTGG	$(GAGT)_{13}$	113–139	4	0.62
	R: GACAGAGACATGCACACACG				
GOBS55	F: ACAGCATTTGTGCATGAACC	$(ACAT)_6$	148–160	5	0.74
	R: GCATACCAGTGGGCATAACG				
GOBS57	F: TGACGATATCCCGGTGTTGG	$(CTTT)_6$	148–167	4	0.69
	R: GAGCCACCAGTCACGATACC				
GOBS65	F: CAAGCTCCAGTCGTCTGTCC	$(ACAG)_8$	198–204	5	0.78
	R: GTTGGGCTGGGTCCATATCC				
GOBS72	F: GGATCCCGACTCTTTGACCC	$(TCTT)_7$	227–247	7	0.84
	R: AGTTCCATTTATTCCCGTTGGG				
GOBS73	F: TCAGTCATGATGGGAGAGAACC	$(GAAA)_8$	231–241	5	0.72
	R: ACCAAGCCATATAACAACCC				
GOBS74	F: CGGGATACAAGGACGATCGG	$(CAGG)_7$	230–245	5	0.74
	R: AAGATCCGAGTGTGGTGTGG				

[a]GenBank accession number: GOBS4–GOBS74: OL630743–OL630770.
[b]Number of alleles.
[c]Genetic diversity (haploid).

that had more than eight repeats. More recently, whole-genome sequencing has increased the ability to find larger numbers of microsatellite regions with a higher number of repeat motifs (Cai et al., 2019; Owati et al., 2019; Si et al., 2019; Varady et al., 2019). In our study, we used a genomic-based approach to identify a total of 3256 di-, tri-, and tetranucleotide repeats as these are the most numerous microsatellite repeats and are used most commonly in population studies. So that many of the smaller repeats that were detected in the preliminary analysis were excluded, and to still yield many potentially informative microsatellites, we set our minimum repeat sampling threshold at greater than 8 for di-, 7 for tri-, and 6 for tetranucleotide repeats.

Primers were designed to amplify *G. obscura* DNA microsatellite regions. We initially screened 75 randomly selected microsatellite markers against three isolates of *G. obscura*, resulting in 100% amplification in at least one isolate. Whole-genome sequencing approach to microsatellite marker development generally results in greater than 80% positive amplification (Cai et al., 2013; Mercière et al., 2015; Schoebel, Jung, et al., 2013; Si et al., 2019; Varady et al., 2019; Zhang et al., 2018). Polymorphic alleles are more difficult to predict and generally range from 10% to 70% of amplicons (Cai et al., 2013; Mercière et al., 2015; Schoebel, Jung, et al., 2013; Si et al., 2019; Zhang et al., 2018). Our results showed that 48% of the microsatellite markers produced

polymorphic amplicons and could be of use in population genetic studies.

Since our goal was to identify microsatellite markers that only amplify *G. obscura* individuals, we tested a subset of the markers with polymorphic amplicons against 12 *Geosmithia* or former *Geosmithia* spp. Of the 28 microsatellite markers tested, we found only 5 to be *G. obscura* specific. When DNA from *R. argillacea* was tested, amplicons of the expected size were obtained using 21 of the microsatellite markers; however, 7 of these only amplified *R. argillacea* in addition to *G. obscura*. In all cases, the amplicons produced for *R. argillaceae* had a much lower RFU (less than 500, of which 3 were below 200 but above our threshold of 100) than the ones produced from *G. obscura* isolates. This low rate of amplification in *R. argillacea* could indicate false positives based on our cut-off threshold. A cut-off threshold is often not reported, though Mercière et al. (2015) set a cutoff at 200 RFU to score amplicons as positive, which if adopted in this study would remove 3 of the positive results we reported. Nine microsatellite markers amplified products in *G. morbida* that were within the expected size range of the *G. obscura* amplicon, but the RFU was generally less than 1000, while the amplicons obtained when using *G. obscura* DNA had a much higher RFU, 2× to 5× higher. To further examine cross-amplification between *G. morbida* and *G. obscura*, we used previously published *G. morbida* microsatellite markers (Hadziabdic et al., 2011) to screen the same 12 *Geosmithia* or

TABLE 4 Cross-amplification of 28 microsatellite markers from *Geosmithia obscura*.

	GOB-S4	GOB-S9	GOB-S10	GOB-S11	GOB-S12	GOB-S13	GOB-S16	GOB-S18	GOB-S20	GOB-S21	GOB-S26	GOB-S31	GOB-S38	GOB-S41	GOB-S43	GOB-S44	GOB-S45	GOB-S46	GOB-S47	GOB-S50	GOB-S51	GOB-S53	GOB-S55	GOB-S57	GOB-S65	GOB-S72	GOB-S73	GOB-S74
Geosmithia lavendula	−	−	−	−	−	−	+	−	−	−	−	−	−	−	−	−	−	−	−	−	−	−	−	−	−	−	−	−
G. lavendula CBS344.49	−	−	−	−	−	−	−	−	−	−	−	−	−	−	−	−	−	−	−	−	−	−	−	−	−	−	−	−
G. morbida GM10	−	−	−	−	−	−	−	+	−	−	−	−	−	−	−	−	−	−	−	−	+	−	−	−	−	−	−	−
G. morbida GM17	−	−	−	−	−	−	−	−	−	−	−	−	−	−	−	−	−	−	−	−	−	−	−	−	−	−	−	−
G. morbida GM182	−	−	−	−	−	−	+	+	+	−	−	−	−	−	−	−	−	−	−	−	−	−	−	−	−	−	−	−
G. morbida GM246	−	−	−	−	−	−	−	+	−	−	−	−	−	−	−	−	−	−	−	−	+	−	−	−	−	−	−	−
G. morbida GM249	+	−	−	−	−	−	−	−	−	+	−	+	−	−	−	−	−	+	−	−	−	−	−	−	+	−	−	−
G. morbida GM250	+	−	−	−	−	−	+	−	−	+	−	+	−	−	−	−	−	+	−	−	−	−	−	−	+	−	−	−
G. pallida 6LN5	+	−	−	−	−	−	−	−	−	−	−	−	−	−	−	−	−	−	−	−	+	−	−	−	−	−	−	+
G. pallida 9730	−	−	−	−	−	−	−	−	−	−	−	−	−	−	−	−	−	−	−	−	−	−	−	−	−	−	−	+
G. pallida 9737	−	−	−	−	−	−	−	−	−	−	−	−	−	−	−	−	−	−	−	−	−	−	−	−	−	−	−	+
G. pallida CBS260.33	+	−	−	−	−	−	−	−	−	−	+	−	−	−	−	−	−	−	−	−	−	−	−	−	−	−	−	−
G. putterelli NRRL 2024	+	−	−	+	−	−	−	+	−	−	+	−	−	−	−	−	−	−	−	−	−	−	−	−	−	−	−	+
G. sp 10 11LE1	−	−	−	−	−	+	−	−	−	−	−	−	−	−	−	−	−	+	−	−	−	+	−	−	−	−	−	−
G. sp 2 3BHS13	−	−	−	−	−	−	−	−	−	−	−	−	−	−	−	−	−	−	−	−	−	−	−	−	−	−	−	+
G. sp 2 K1W1	+	−	−	−	−	−	−	−	−	−	−	−	−	−	−	−	−	−	−	−	+	−	−	−	−	−	−	+
G. sp 2 LS1XB	+	−	−	−	−	−	−	−	−	−	−	−	−	−	−	−	−	−	−	−	−	−	−	−	−	−	−	+
G. sp 21 LS5XB	+	−	−	−	−	−	−	−	−	−	−	−	−	−	−	−	−	−	−	−	−	−	−	−	−	−	−	−
G. sp 23 4LW11	−	−	−	−	−	−	−	−	−	−	−	−	−	−	−	−	−	−	−	−	−	−	−	−	−	−	−	−
G. sp 23 4MN3	+	−	−	−	−	−	−	+	−	+	−	−	−	−	−	−	−	−	−	−	−	−	−	−	−	−	−	+
G. sp 41 18MN2	−	−	−	−	−	−	−	+	−	−	−	−	−	−	−	−	−	−	−	−	−	−	−	−	−	−	−	+
G. sp 41 4BE20	−	−	−	−	−	−	−	+	−	−	−	−	+	−	−	−	−	−	−	−	−	−	−	−	+	−	−	+
G. sp 41 6ME1	−	−	−	−	−	−	−	+	−	−	−	−	+	−	−	−	−	−	−	−	−	−	−	−	−	−	−	+
G. sp 41 8BN26	−	−	−	−	−	−	+	−	−	−	−	−	+	−	−	−	−	−	−	−	−	−	−	−	−	−	−	+
Penicillium namyslowskii CBS686.85	−	−	−	+	−	−	−	−	−	−	−	−	−	−	−	+	−	−	−	−	−	−	−	−	−	−	−	−
Rasamsonia argillaceae	+	−	−	+	+	+	−	+	−	+	+	+	+	−	−	+	+	+	+	−	+	+	+	+	+	+	+	−

(Continues)

TABLE 4 (Continued)

	GOB-S4	GOB-S9	GOB-S10	GOB-S11	GOB-S12	GOB-S13	GOB-S16	GOB-S18	GOB-S20	GOB-S21	GOB-S26	GOB-S31	GOB-S38	GOB-S41	GOB-S43	GOB-S44	GOB-S45	GOB-S46	GOB-S47	GOB-S50	GOB-S51	GOB-S53	GOB-S55	GOB-S57	GOB-S65	GOB-S72	GOB-S73	GOB-S74
Talaromyces viridulus CBS252.87	–	–	–	–	–	+	–	–	–	–	–	–	–	–	–	–	–	–	–	–	–	–	–	–	–	–	–	–
Geosmithia obscura (positive control) 18BS1	+	+	+	+	+	+	+	+	+	+	+	+	+	+	+	+	+	+	+	+	+	+	+	+	+	+	+	+

former *Geosmithia* spp. and *G. obscura*, as above. This effort resulted in only one microsatellite marker, GSA0051, generating an amplicon of expected size when using nine isolates of *G. obscura* DNA with an RFU similar to the amplicon from *G. morbida* DNA.

In general, the cross-transferability of microsatellite regions and flanking primers is low in fungi, especially across genera (Cai et al., 2013; Dutech et al., 2007; Mercière et al., 2015). When characterizing markers for use in molecular identification, detection, or species barcoding, cross-transferability that may confound result interpretation is undesirable. In a cross-transferability study by Du et al. (2019), a high percentage of microsatellite regions were amplified across six species of morel fungi (*Morchella* sp.), suggesting that these regions have been conserved in *Morchella* through evolutionary processes. For those species that were more closely related, there was a higher likelihood that the microsatellite markers would amplify a product of the expected length. *Morchella* species can hybridize and this may contribute to the high level of cross-amplification. Sexual reproduction, although suspected, has not been reported in *Geosmithia* species; therefore, hybridization between species is unlikely. Horizontal transfer of genes between species has occurred when fungi coincide within a common host. For example, the *cu* gene from *Ophiostoma novo-ulmi* was identified in *Geosmithia* sp. 5 that was coinhabiting in *Ulmus* sp. (Bettini et al., 2014). Many of our Tennessee isolates were collected in the same geographic area and could incur some horizontal transfer between species occupying the same host niche, and thus may explain some of the positive cross-amplification that was observed.

Microsatellite development for the fungal pathogen *Ganoderma bonensis* based on its genome resulted in 16 out of 17 microsatellite markers that also amplified alleles of the same size in a closely related species, *Ganoderma resinaceum* (Mercière et al., 2015). When the microsatellite regions were screened against the genome of a third, more distantly related species, *Ganoderma lucidum*, they could not identify motifs that matched the specific microsatellite markers. We screened nine *Geosmithia* species and three fungal species that formerly had been classified as *Geosmithia*. *Rasamsonia argillacea* amplified alleles of similar size in 21 out of 28 microsatellite markers; however, many of these alleles could have been false positives. No other fungal species consistently amplified alleles, which is consistent with genetic differences between the species (Kolarik et al., 2005, 2017).

Schoebel, Jung et al. (2013) examined the cross transferability of microsatellite markers within and between clades of *Phytophthora* species. They found that microsatellite markers designed for specific species produced amplicons at the highest rate by that species, but were amplified less frequently by other species within the same clade. Amplification between clades did occur, but at low frequency, and many products were not of the expected size or inconsistent for a species. We found inconsistent amplification when using DNA from species other than *G. obscura*. Many of the species that yielded an amplicon had very low RFU values (100–500) compared to *G. obscura* or the size range was not within the range expected for *G. obscura*.

The goals for developing SSR markers for *G. obscura* included species identification and potential detection in heterogeneous samples as well as for future population studies of this species. We developed five microsatellite markers with consistent and easily distinguishable polymorphic alleles that are specific to *G. obscura* and can be used for species identification and species detection. For population studies, the recommended number of polymorphic alleles is between 8 and 16 (Du et al., 2019; Schoebel, Brodbeck, et al., 2013). We achieved this goal with all 28 of the microsatellite markers that we tested; of these, 26 markers consistently amplified products yielding a high RFU value. Population studies conducted using strains that have been positively identified using ITS or other means do not require species-specific microsatellite markers, provided that the microsatellite markers used the amplify regions that are polymorphic within the target species.

The diagnostic capabilities of the markers developed here will support/inform several critical next steps for addressing our knowledge gaps about the genus *Geosmithia* and *G. obscura* specifically. Specific markers will be used to guide screening efforts that will assist with additional *G. obscura* isolate recovery, which is needed to validate the potential for pathogenicity. Enhanced screening efforts also will help articulate interactions with potential arthropod associates that may be serving as vectors for the fungus. Results from such work are expected to provide a benchmark for future population studies and estimates of genetic diversity and spatial distribution within the *Geosmithia* genus.

AUTHOR CONTRIBUTIONS

Grace M. Pietsch: Data curation (lead); formal analysis (equal); investigation (lead); methodology (lead); validation (lead); visualization (lead); writing—original draft (lead). **Romina Gazis**: Investigation (supporting); methodology (supporting); writing—original draft (supporting); writing—review and editing (supporting). **William E. Klingeman**: Conceptualization (lead); data curation (equal); funding acquisition (lead); investigation (supporting); methodology (supporting); project administration (supporting); resources (lead); supervision (lead); validation (equal); visualization (equal); writing—original draft (supporting); writing—review and editing (supporting). **Matthew L. Huff**: Data curation (supporting); formal analysis (supporting); software (lead); writing—review and editing (supporting). **Miroslav Kolarik**: Data curation (supporting); validation (supporting); writing—review and editing (supporting). **Denita Hadziabdic**: Conceptualization (lead); data curation (equal); formal analysis (lead); funding acquisition (equal); investigation (supporting); methodology (supporting); project administration (equal); resources (equal); supervision (supporting); validation (supporting); visualization (supporting); writing—original draft (supporting); writing—review and editing (supporting).

ACKNOWLEDGMENTS

CONFLICTS OF INTEREST

None declared.

DATA AVAILABILITY STATEMENT

The data that supports the findings of this study are openly available in the Dryad repository at https://doi.org/10.5061/dryad.nk98sf7w2.

ETHICS STATEMENT

None required.

ORCID

Romina Gazis http://orcid.org/0000-0002-7979-176X
William E. Klingeman http://orcid.org/0000-0001-6272-0079
Matthew L. Huff http://orcid.org/0000-0001-6760-0762
Margaret E. Staton http://orcid.org/0000-0003-2971-9353
Miroslav Kolarik http://orcid.org/0000-0003-4016-0335
Denita Hadziabdic http://orcid.org/0000-0003-1991-2563

REFERENCES

Andrews, S. (2010). *FastQC: A quality control tool for high throughput sequence data*. Babraham Bioinformatics, Babraham Institute.

Bettini, P. P., Frascella, A., Kolarik, M., Comparini, C., Pepori, A. L., Santini, A., Scala, F., & Scala, A. (2014). Widespread horizontal transfer of the *cerato-ulmin* gene between *Ophiostoma novo-ulmi* and *Geosmithia* species. *Fungal Biology*, 118, 663–674.

Cai, G., Fleury, T. J., & Zhang, N. (2019). Comparative genomics approach to build a genome-wide database of high-quality, informative microsatellite markers: Application on *Phytophthora sojae*, a soybean pathogen. *Scientific Reports*, 9, 7969.

Cai, G., Leadbetter, C. W., Muehlbauer, M. F., Molnar, T. J., & Hillman, B. I. (2013). Genome-wide microsatellite identification in the fungus *Anisogramma anomala* using Illumina sequencing and genome assembly. *PLoS One*, 8, e82408.

Chahal, K., Gazis, R., Klingeman, W., Hadziabdic, D., Lambdin, P., Grant, J., & Windham, M. (2019). Assessment of alternative candidate subcortical insect vectors from walnut crowns in habitats quarantined for Thousand Cankers Disease. *Environmental Entomology*, 48, 882–893.

Chahal, K., Gazis, R. O., Grant, J., Hadziabdic, D., Lambdin, P., Klingeman, W., Paulsen, D., & Windham, M. T. (2017). Potential alternative vectors of *Geosmithia morbida* (Thousand Cankers Disease) in east Tennessee. In *APS Annual Meeting, San Antonio, Texas. Phytopathology*. University of Tennessee.

Du, X. H., Wang, H., Sun, J., Xiong, L., & Yu, J. (2019). Hybridization, characterization and transferability of SSRs in the genus *Morchella*. *Fungal Biology*, 123, 528–538.

Dutech, C., Enjalbert, J., Fournier, E., Delmotte, F., Barres, B., Carlier, J., Tharreau, D., & Giraud, T. (2007). Challenges of microsatellite isolation in fungi. *Fungal Genetics and Biology*, 44, 933–949.

Freeland, E. (2012). *Intraspecific variability of Geosmithia morbida the causal agent of Thousand Cankers Disease, and effects of temperature, isolate and host family (Juglens nigra) on canker development* (Master of Science). Colorado State University. https://mountainscholar.org/

bitstream/handle/10217/65340/Freeland_colostate_0053N_10946.pdf

Gardes, M., & Bruns, T. D. (1993). ITS primers with enhanced specificity for basidiomycetes-application to the identification of mycorrhizae and rusts. *Molecular Ecology*, 2, 113–118.

Gazis, R., Kuo, A., Riley, R., Labutti, K., Lipzen, A., Lin, J., Amirebrahimi, M., Hesse, C. N., Spatafora, J. W., Henrissat, B., Hainaut, M., Grigoriev, I. V., & Hibbett, D. S. (2016). The genome of *Xylona heveae* provides a window into fungal endophytism. *Fungal Biology*, 120, 26–42.

Gazis, R., Poplawski, L., Klingeman, W., Boggess, S. L., Trigiano, R. N., Graves, A. D., Seybold, S. J., & Hadziabdic, D. (2018). Mycobiota associated with insect galleries in walnut with Thousand Cankers Disease reveals a potential natural enemy against *Geosmithia morbida*. *Fungal Biol*, 122, 241–253.

Hadziabdic, D., Vito, L. M., Windham, M. T., Pscheidt, J. W., Trigiano, R. N., & Kolarik, M. (2014). Genetic differentiation and spatial structure of *Geosmithia morbida*, the causal agent of Thousand Cankers Disease in black walnut (*Juglans nigra*). *Current Genetics*, 60, 75–87.

Hadziabdic, D., Wadl, P. A., Vito, L. M., Boggess, S. L., Scheffler, B. E., Windham, M. T., & Trigiano, R. N. (2011). Development and characterization of sixteen microsatellite loci for *Geosmithia morbida*, the causal agent of thousand canker disease in black walnut (*Juglans nigra*). *Conservation Genetics Resources*, 4, 287–289.

Houbraken, J., Spierenburg, H., & Frisvad, J. C. (2012). *Rasamsonia*, a new genus comprising thermotolerant and thermophilic *Talaromyces* and *Geosmithia* species. *Antonie Van Leeuwenhoek*, 101, 403–421.

Huang, Y. T., Kolarik, M., Kasson, M. T., & Hulcr, J. (2017). Two new *Geosmithia* species in G. *pallida* species complex from bark beetles in eastern USA. *Mycologia*, 109, 790–803.

Huang, Y. -T., Skelton, J., Johnson, A. J., Kolařík, M., & Hulcr, J. (2019). *Geosmithia* species in southeastern USA and their affinity to beetle vectors and tree hosts. *Fungal Ecology*, 39, 168–183.

Jiang, H., Lei, R., Ding, S. -W., & Zhu, S. (2014). Skewer: A fast and accurate adapter trimmer for next-generation sequencing paired-end reads. *BMC Bioinformatics*, 15, 182.

Kolarik, M., Freeland, E., Utley, C., & Tisserat, N. (2011). *Geosmithia morbida* sp. nov., a new phytopathogenic species living in symbiosis with the walnut twig beetle (*Pityophthorus juglandis*) on *Juglans* in USA. *Mycologia*, 103, 325–332.

Kolarik, M., Hulcr, J., Tisserat, N., DE Beer, W., Kostovcik, M., Kolarikova, Z., Seybold, S. J. & Rizzo, D. M. (2017). *Geosmithia* associated with bark beetles and woodborers in the western USA: Taxonomic diversity and vector specificity. *Mycologia*, 109, 185–199.

Kolarik, M., & Jankowiak, R. (2013). Vector affinity and diversity of *Geosmithia* fungi living on subcortical insects inhabiting Pinaceae species in central and northeastern Europe. *Microbial Ecology*, 66, 682–700.

Kolarik, M., Kubatova, A., Van Cepicka, I., Pazoutova, S., & Srutka, P. (2005). A complex of three new white-spored, sympatric, and host range limited *Geosmithia* species. *Mycological Research*, 109, 1323–1336.

Kolařík, M., Kostovčík, M., & Pažoutová, S. (2007). Host range and diversity of the genus *Geosmithia* (Ascomycota: Hypocreales) living in association with bark beetles in the Mediterranean area. *Mycological Research*, 111, 1298–1310.

Kolařík, M., Kubátová, A., Hulcr, J., & Pažoutová, S. (2008). *Geosmithia* fungi are highly diverse and consistent bark beetle associates: Evidence from their community structure in temperate Europe. *Microbial Ecology*, 55, 65–80.

Li, H. (2015). BFC: Correcting Illumina sequencing errors. *Bioinformatics*, 31, 2885–2887.

Lynch, S. C., Wang, D. H., Mayorquin, J. S., Rugman-Jones, P. F., Stouthamer, R., & Eskalen, A. (2014). First report of *Geosmithia pallida* causing Foamy Bark Canker, a new disease on Coast Live Oak (*Quercus agrifolia*), in association with *Pseudopityophthorus pubipennis* in California. *Plant Disease*, 98, 1276.

Mercière, M., Laybats, A., Carasco-Lacombe, C., Tan, J. S., Klopp, C., Durand-Gasselin, T., Alwee, S. S. R. S., Camus-Kulandaivelu, L., & Breton, F. (2015). Identification and development of new polymorphic microsatellite markers using genome assembly for *Ganoderma boninense*, causal agent of oil palm basal stem rot disease. *Mycological Progress*, 14, 103.

Morgulis, A., Gertz, E. M., Schäffer, A. A., & Agarwala, R. (2006). A fast and symmetric DUST implementation to mask low-complexity DNA sequences. *Journal of Computational Biology*, 13, 1028–1040.

Oren, E., Klingeman, W., Gazis, R., Moulton, J., Lambdin, P., Coggeshall, M., Hulcr, J., Seybold, S. J., & Hadziabdic, D. (2018). A novel molecular toolkit for rapid detection of the pathogen and primary vector of Thousand Cankers Disease. *PLoS One*, 13, e0185087.

Owati, A., Agindotan, B., & Burrows, M. (2019). First microsatellite markers developed and applied for the genetic diversity study and population structure of *Didymella pisi* associated with ascochyta blight of dry pea in Montana. *Fungal Biology*, 123, 384–392.

Peakall, R., & Smouse, P. E. (2012). GenAlEx 6.5: Genetic analysis in Excel. Population genetic software for teaching and research—An update. *Bioinformatics*, 28, 2537–2539.

Rozen, S., & Skaletsky, H. (2000). Primer3 on the WWW for general users and for biologist programmers. In S. Misener, & S. A. Krawetz (Eds.), *Methods in Molecular Biology*. Humana Press Inc.

Schoebel, C. N., Brodbeck, S., Buehler, D., Cornejo, C., Gajurel, J., Hartikainen, H., Keller, D., Leys, M., Ricanova, S., Segelbacher, G., Werth, S., & Csencsics, D. (2013). Lessons learned from microsatellite development for nonmodel organisms using 454 pyrosequencing. *Journal of Evolutionary Biology*, 26, 600–611.

Schoebel, C. N., Jung, E., & Prospero, S. (2013). Development of new polymorphic microsatellite markers for three closely related plant-pathogenic *Phytophthora* species using 454-pyrosequencing and their potential applications. *Phytopathology*, 103, 1020–1027.

Schuelke, T. A., Westbrook, A., Broders, K., Woeste, K., & Macmanes, M. D. (2016). De novo genome assembly of *Geosmithia morbida*, the causal agent of Thousand Cankers Disease. *PeerJ*, 4, e1952.

Si, E., Meng, Y., Ma, X., Li, B., Wang, J., Ren, P., Yao, L., Yang, K., Zhang, Y., Shang, X., & Wang, H. (2019). Development and characterization of microsatellite markers based on whole-genome sequences and pathogenicity differentiation of *Pyrenophora graminea*, the causative agent of barley leaf stripe. *European Journal of Plant Pathology*, 154, 227–241.

Simpson, J. T., Wong, K., Jackman, S. D., Schein, J. E., Jones, S. J., & Birol, I. (2009). ABySS: A parallel assembler for short read sequence data. *Genome Research*, 19, 1117–1123.

Six, D. L., Stone, W. D., De Beer, Z. W., & Woolfolk, S. W. (2009). *Ambrosiella beaveri*, sp. nov., associated with an exotic ambrosia beetle, *Xylosandrus mutilatus* (Coleoptera: Curculionidae, Scolytinae), in Mississippi, USA. *Antonie Van Leeuwenhoek*, 96, 17–29.

Stackhouse, T., Boggess, S. L., Hadziabdic, D., Trigiano, R. N., Ginzel, M. D., & Klingeman, W. E. (2021). Conventional gel electrophoresis and TaqMan probes enable rapid confirmation of Thousand Cankers Disease from diagnostic samples. *Plant Disease*, 105, 3171–3180.

Staton, M. E., & Ficklin, S. 2018. *Finding SSRs—Findssrs_altered.pl*. Github repository: https://github.com/statonlab/Finding-SSRs/blob/master/findSSRs_altered.pl.

Strzalka, B., Kolarik, M., & Jankowiak, R. (2021). *Geosmithia* associated with hardwood-infesting bark and ambrosia beetles, with the description of three new species from Poland. *Antonie Van Leeuwenhoek*, 114, 169–194.

Tisserat, N., Cranshaw, W., Leatherman, D., Utley, C., & Alexander, K. (2009). Black walnut mortality in Colorado caused by the walnut

twig beetle and Thousand Cankers Disease. *Plant Health Progress*, *10*, 10.

Untergasser, A., Cutcutache, I., Koressaar, T., Ye, J., Faircloth, B. C., Remm, M., & Rozen, S. G. (2012). Primer3—New capabilities and interfaces. *Nucleic acids research*, *40*, e115–e115.

Varady, E. S., Bodaghi, S., Vidalakis, G., & Douhan, G. W. (2019). Microsatellite characterization and marker development for the fungus *Penicillium digitatum*, causal agent of green mold of citrus. *Microbiology Open*, *8*(7), e788.

White, T. J., Bruns, T. D., Lee, S. B., & Taylor, J. W. (1990). Amplification and direct sequencing of fungal ribosomal RNA genes for phylogenetics. In M. A. Innis, D. H. Gelfand, J. J. Sninsky, & T. J. White (Eds.), *PCR protocols: A guide to methods and applications* (pp. 315–322). Academic Press.

Zerillo, M. M., Ibarra Caballero, J., Woeste, K., Graves, A. D., Hartel, C., Pscheidt, J. W., Tonos, J., Broders, K., Cranshaw, W., Seybold, S. J., & Tisserat, N. (2014). Population structure of *Geosmithia morbida*, the causal agent of Thousand Cankers Disease of walnut trees in the United States. *PLoS One*, *9*, e112847.

Zhang, Y., He, W., & Yan, D. H. (2018). Genomewide identification and development of microsatellite markers for *Marssonina brunnea* and their applications in two populations. *Forest Pathology*, *48*, e12433.
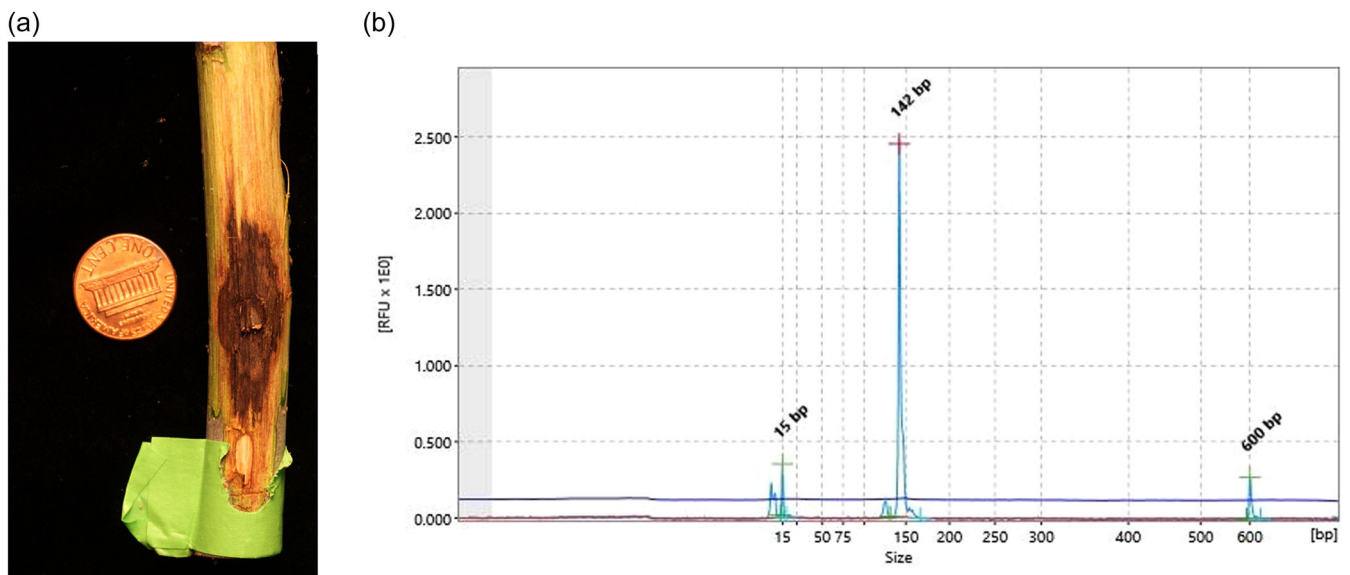
APPENDIX

Figure A1

(a)

(b)

FIGURE A1 (a) An example of an approximately 190 mm² canker formed within the phloem tissue of a 5-year-old *Juglans nigra* L. tree sampled 14 days after inoculation with *Geosmithia obscura* isolate 6BE2. (b) An example of the QIAxcel electropherogram (142 bp peak) of a positive *G. obscura* 6BE2 sample amplified using the GOBS10 microsatellite marker.